



Cite this: *Green Chem.*, 2023, **25**, 5634

## Sequential extraction of hemicelluloses by subcritical water improves saccharification of hybrid aspen wood grown in greenhouse and field conditions†

Pramod Sivan, †<sup>a</sup> Emilia Heinonen, †<sup>a,b</sup> Madhavi Latha Gandla, <sup>c</sup> Amparo Jiménez-Quero, <sup>a</sup> Hüsamettin Deniz Özeren, <sup>a</sup> Leif J. Jönsson, <sup>c</sup> Ewa J. Mellerowicz<sup>d</sup> and Francisco Vilaplana \*<sup>a,b</sup>

Fast growing hardwoods are one of the major renewable resources available to produce bio-based materials, platform chemicals and biofuels. However, the industrial processing of lignocellulosic biomass is hindered by the complex molecular structure of the cell wall components and their supramolecular organization. This highlights the necessity of improving green processing strategies to enhance biomass conversion to valuable products from industrial wood production species. In the present study, we implemented a hydrothermal step by sequential subcritical water (SW) in aspen wood prior to saccharification and validated the process for trees grown in greenhouse and field conditions. Subcritical water enables extraction of non-cellulosic cell wall polysaccharides in native polymeric form. A major part of the pectic fraction was easily extracted within the first 10 min, while acetylated xylan was enriched in the subsequent extracts after 20- and 30-min rounds. Prolonged extraction (above 60 min) resulted in partial deacetylation and a reduction of the molar mass of xylan. The analysis of the residues enriched with cellulose and lignin showed several micromorphological changes caused by subcritical water treatment, such as an increased porosity, a loosening of the fibre matrix and a decrease in the macrofibrillar dimensions. These morphological and molecular changes in the organization of cell wall polymers after SW treatment significantly enhanced saccharification yields compared to those of non-treated aspen wood chips from both field and greenhouse conditions. Our study demonstrates that SW can be implemented as pretreatment prior to saccharification reducing the requirements for chemical acid pretreatments. This process enables the extraction of native non-cellulosic cell wall polymers for potential material applications and promotes the subsequent biochemical conversion of the residual biomass into fermentable sugars and platform chemicals in future biorefineries.

Received 29th March 2023,  
 Accepted 15th June 2023  
 DOI: 10.1039/d3gc01020a  
[rsc.li/greenchem](http://rsc.li/greenchem)

## Introduction

Lignocellulosic biomass represents the most abundant renewable resource on Earth for the sustainable production of eco-friendly materials,<sup>1,2</sup> platform chemicals, and energy with

almost CO<sub>2</sub>-neutral balance to slow down the global trend of CO<sub>2</sub> increase.<sup>3,4</sup> Lignocellulose is a heterogenous biocomposite composed of cellulose, hemicelluloses, pectins and lignin, tightly linked to each other through covalent linkages and non-covalent interactions. Cellulose has been traditionally used in the paper and pulp sectors, and through its nanotechnological modification it has the potential to substitute fossil-based structural polymers in all imaginable sectors, including electronics, energy storage and biomedical applications.<sup>5-7</sup> Lignin is the major bio-based source of aromatics through thermal and catalytic valorization,<sup>8,9</sup> and can be largely utilized as source of platform chemicals, polymers,<sup>10</sup> and for the synthesis of lignin-based nanoparticles.<sup>11</sup> Traditionally, hemicelluloses and pectins have been underexploited compared to the other lignocellulosic components, as they are largely degraded in the harsh conditions of the traditional pulp and

<sup>a</sup>Division of Glycoscience, Department of Chemistry, KTH Royal Institute of Technology, AlbaNova University Centre, 106 91 Stockholm, Sweden.

E-mail: [franvila@kth.se](mailto:franvila@kth.se)

<sup>b</sup>Wallenberg Wood Science Centre, KTH Royal Institute of Technology, 100 44 Stockholm, Sweden

<sup>c</sup>Department of Chemistry, Umeå University, 901 87 Umeå, Sweden

<sup>d</sup>Umeå Plant Science Centre, Swedish University of Agricultural Sciences, Department of Forest Genetics and Plant Physiology, 901 83 Umeå, Sweden

† Electronic supplementary information (ESI) available. See DOI: <https://doi.org/10.1039/d3gc01020a>

‡ These authors contributed equally to this work.



paper processes. However, these polymers have large potential to be used for production of many high value products such as surface modifiers and texturing agents,<sup>6</sup> packaging materials<sup>7,12</sup> and precursors of bio-based plastics.<sup>13</sup>

Lignocellulose recalcitrance has been the major challenge that hinders fractionation efficiency and conversion of biomass into derived bioproducts.<sup>14,15</sup> Recalcitrance is conferred by multiple factors such as interactions among cell wall components, cellulose fibrillar characteristics such as crystallinity, microfibril diameter, and coalescence into macrofibrillar aggregates.<sup>2,14,15</sup> Hemicelluloses and pectins contribute to lignocellulose recalcitrance due to their interactions with both cellulose microfibrils and lignin, acting as a transition phase between these components and as a physical barrier for the enzymatic hydrolysis of cellulose fibres.<sup>16,17</sup> These important biological functions of hemicelluloses and pectins are regulated during biosynthesis and attributed to molecular features such as degree of polymerization, substitution pattern and crosslinking initiation sites.<sup>14,18</sup> The morphological features of cellulose microfibrils (e.g. their diameter) and their aggregation are believed to be modulated through supramolecular interactions (both hydrogen bonding and van der Waals interactions) with hemicellulosic xylans and glucomannans at the microfibril surfaces; therefore, disruption of these aggregated forms constitutes a key target for increasing efficiency of biochemical conversion processes.<sup>14</sup> This suggests the potential benefits of implementing hemicellulose-first approaches in biorefinery settings to increase the efficacy of biochemical conversion of lignocellulose.

Recent developments in the extraction of hemicellulose and lignin using sequential subcritical water extraction (SWE) with a buffered extraction solvent has provided novel insights on the native structure, composition and interactive domains of hemicelluloses and their lignin complexes (LCCs) from spruce (softwood) and birch (hardwood).<sup>2,19</sup> SWE is a green extraction method based on pressurized water as a solvent under increased temperature, which facilitates the isolation of different pectin and hemicellulose populations depending on their recalcitrance in the lignocellulose network. SWE (also referred to as pressurized hot-water extraction or hydrothermal extraction) can be scaled up and run in both batch and semi-continuous mode.<sup>20,21</sup> The different extractability of pectin and hemicellulose populations and the control of extraction times enable the targeted isolation of mannan and xylan populations with controlled acetylation and (in case of xylan) glucuronation.<sup>2,19</sup> Moreover, the use of controlled buffered pH conditions during SWE preserves the acetylation in the extracted hemicelluloses, preventing its release into the aqueous phase and the occurrence of acid-induced autohydrolysis,<sup>2,22</sup> as opposed to other studies where unbuffered conditions resulted in drastic depolymerization of the hemicelluloses and release of sugar monomers and oligomers.<sup>20</sup> Hardwoods represent one of the most abundant resources for lignocellulose based biorefineries and biobased materials. *Populus* sp. trees including hybrid aspens and poplars are high yielding hardwood tree species with glucan

content ranging from 40–62%, xylan content from 14–24% and lignin content 15–29% of the total dry weight and considered to be one of the most promising tree crops for production of bioenergy feedstock in short-rotation plantations.<sup>23</sup> Being a model plant for hardwood species, *Populus* is extensively used for genetic engineering approaches to improve lignocellulose properties.<sup>24</sup> The genetically engineered *Populus* trees are usually tested first under greenhouse conditions and then selected genotypes are evaluated under field conditions. In the present study, we have compared the potential of SWE for yielding high molecular weight hemicelluloses and pectins from the wood of hybrid aspen (*Populus tremula* L. X *tremuloides* Michx) trees. The structural changes in the extracted fractions have been monitored to identify links between the molecular structure and extractability of polymers. The potential of SWE process as an integrated hemicellulose-first approach prior to saccharification in biorefinery applications has been evaluated and validated with aspen trees grown in greenhouse and field conditions.

## Materials and methods

### Plant material

Hybrid aspen (*Populus tremula* L. X *tremuloides* Michx.), clone T89, was used for all experiments. Greenhouse grown trees were harvested after 13 weeks of cultivation in conditions previously described.<sup>20</sup> Field grown trees were harvested in July 2014 after five growth seasons in the field as described previously.<sup>25</sup> The wood from greenhouse-grown trees was dissected and freeze-dried<sup>20</sup> whereas the wood from the field-grown trees was dissected and dried at 60 °C.<sup>25</sup>

### Chemicals

All chemicals, analytical standards and reagents were from Sigma-Aldrich (Stockholm, Sweden) unless otherwise stated.

### Implementation of the extraction and saccharification process

**Preparation of wood powder.** Dried aspen wood of individual eight and 16 trees from greenhouse and field conditions, respectively, were ground to a rough powder in the Cutting Mill SM 300 using 2 mm sieve (Retsch, Haan, Germany). Rough powder was then sieved on vibratory sieve shaker AS 200 (Retsch) and divided into the fractions of particle size: <50 µm, 50–100 µm, 100–500 µm and >500 µm. The wood powder of <50 µm fraction and 100–500 µm fraction was then combined for all trees either grown in the greenhouse or in the field and unless otherwise stated, the 100–500 µm fraction was used for further analyses.

**Subcritical water extraction.** Four wood powder samples (2 g) from each type of material were extracted in 0.2 M formate buffer, pH 5.0, at 170 °C and 100 bar with an accelerated solvent extractor (ASE-300, Dionex, USA). Extraction proceeded in 4 steps with residence times of 10, 20, 30 and 60 min. The extraction conditions (temperature, pH and duration) were implemented following previously optimized con-

ditions for hardwoods and softwoods.<sup>2,19</sup> Salts and low molecular weight compounds were removed from extracts by dialysis using Spectra/Por 3 membranes (Spectrum, USA), after which the extracted polymers were freeze-dried and weighted prior to analysis.

**Analytical saccharification with and without acid pre-treatment.** Greenhouse- and field grown ground and sieved wood was subjected to acid pretreatment in triplicate, using 50 mg of dry (based on HG63 moisture analyzer) powder and an Initiator single-mode microwave instrument (Biotage, Uppsala, Sweden) as previously described.<sup>26</sup> Enzymatic hydrolysis was performed using either 50 mg of dry wood powder, 50 mg of dry residue of SWE process, or the residue of acid pretreatment, according to the method previously described.<sup>26</sup> Each processed SWE replicate, wood powder, and acid pretreated wood powder was analyzed in triplicate. Enzymatic hydrolysis was performed at 45 °C using 5 mg of the liquid enzyme preparation Cellic CTec-2 (obtained from Sigma-Aldrich, St Louis, MO, USA). Samples were collected after 2 h and 72 h of incubation. The glucose production rate was estimated by using an Accu-Chek ®Aviva glucometer (Roche Diagnostics Scandinavia AB, Bromma, Sweden) after calibration with a set of glucose standard solutions for samples withdrawn after 2 h. For samples collected after 72 h, the yield of monosaccharides, including arabinose, galactose, glucose, xylose and mannose, was quantified by using a high-performance anion-exchange chromatography (HPAEC) system with pulsed amperometric detection (Ion Chromatography System ICS-5000, Dionex, Sunnyvale, CA, USA).<sup>27</sup>

### Characterization of the extracts

**Monosaccharide analysis.** The sugar composition of sequential extracts containing non-cellulosic polysaccharides was determined following acidic methanolysis.<sup>28</sup> In brief, 1 mg of freeze-dried extract was incubated with 1 ml of 2 M HCl in dry methanol for 5 h at 100 °C. Samples were then neutralized with pyridine, dried under stream of air and further hydrolyzed with 2 M Trifluoroacetic acid (TFA) at 120 °C for 1 h. The samples were then air dried and dissolved in water for sugar analysis by high performance anion exchange chromatography with pulsed amperometric detection (HPAEC-PAD) (ICS-6000 DC, Dionex) equipped with a CarboPac PA1 column (4 × 250 mm, Dionex) at 30 °C using the eluent gradients previously reported.<sup>29</sup> Samples were run in triplicates.

The starting wood powder material and the SWE residues were subjected to a two-step sulfuric hydrolysis for total sugar compositional analysis considering cellulose and non-cellulosic polysaccharides.<sup>30</sup> In brief, 1 mg of starting wood biomass or residue was incubated with 125 µL of 72% H<sub>2</sub>SO<sub>4</sub> at room temperature for 3 h, then diluted with 1375 µL of deionized water and subsequently incubated at 100 °C for 3 hours. Hydrolysates were diluted with MilliQ water and further filtered through 0.2 mm syringe filter (Chromacol 17-SF-02-N) into HPAEC-PAD vials and analyzed as above. Quantification of monosaccharide composition (monomeric form) was performed by standard calibration of ten monosaccharides (Ara,

Rha, Fuc, Xyl, Man, Gal, Glc, GalA, 4-O-MeGlcA and GlcA) with concentrations between 0.005–0.1 g L<sup>-1</sup>. All experiments were conducted in triplicates.

**Starch content.** Soluble sugars were extracted from wood powder and dried extracts with 80% and 70% ethanol as previously described.<sup>31,32</sup> Starch was analyzed in the residue from ethanol extraction by gelatinization and enzymatic degradation.<sup>33,34</sup> For gelatinization, samples were incubated in 0.1 M NaOH at 95 °C for 30 minutes. After addition of 8 µL of 0.1 M sodium acetate/NaOH buffer per mg of residue to obtain pH 4.9, the suspensions were digested overnight with a-amylase and a-amyloglucosidase at 37 °C and the glucose content was determined by microplate spectrophotometry at 340 nm (Epoch™, BioTek, Germany).

**Py-GC/MS.** Pyrolysis gas chromatography with mass spectrometry (Py-GC/MS) was performed on wood powder (fraction <50 µm) and on freeze-dried extracts.<sup>26</sup> Fifty µg (± 10 µg) of material was applied to a pyrolyzer equipped with an autosampler (PY-2020iD and AS-1020E, Frontier Lab, Japan) connected to a GC/MS (7890A/5975C; Agilent Technologies AB, Sweden) and analyzed as described previously.<sup>22,35</sup>

**Lignin content.** The lignin content of the extracts and residues was measured by acetyl bromide method<sup>31</sup> in duplicates. Samples were incubated in 25% acetyl bromide in glacial acetic acid at 50 °C for 2 h. After addition of 2 M NaOH and 0.5 M hydroxylamine hydrochloride, the samples were diluted with glacial acetic acid. UV absorbance was measured in an ELISA reader at 280 nm. The lignin concentration was estimated from the interpolation of the recorded absorbance against a standard curve from alkaline kraft lignin (Sigma, Germany).

**Acetyl content.** The acetyl content of the extracts and residues was determined in duplicates by saponification and subsequent determination of the released acetic acid by High Pressure Liquid Chromatography with Ultraviolet detector (HPLC-UV). Shortly, about 5 mg of sample was incubated overnight in 0.8 M NaOH at 60 °C with constant mixing. Samples were then neutralized with 37% HCl and filtered through 0.45 mm Chromacol syringe filters (17-SF-02(N), Thermo Fisher Scientific). The acetic acid was detected by UV at 210 nm (HPLC-UV Dionex-Thermofisher Ultimate 3100, USA), after separation with a Rezex ROA-organic acid column (300 × 7.8 mm, Phenomenex, USA) at 50 °C in a 2.5 mM H<sub>2</sub>SO<sub>4</sub> at 0.5 mL min<sup>-1</sup>. Propionic acid was used as an internal standard.

**Molar mass distributions.** The molar mass distributions of the extracts were determined by size exclusion chromatography coupled to refractive index and UV-detectors (SECurity 1260, Polymer Standard Services, Mainz, Germany). The samples were dissolved at 2 mg mL<sup>-1</sup> in dimethyl sulfoxide (DMSO Anhydrous, Sigma-Aldrich) with 0.5% w/w LiBr (Anhydrous free-flowing Redi-Dri, Sigma-Aldrich) at 60 °C, and filtered through 0.45 µm PTFE syringe filters (VWR). The separation was carried through GRAM Analytical columns of 100 and 10 000 Å (Polymer Standard Services, Mainz, Germany) at a flow rate of 0.5 mL min<sup>-1</sup> and 60 °C. The columns were cali-



brated using pullulan standards between 345 and 708 000 Da (Polymer Standard Services, Mainz, Germany).

**Statistical analysis.** Statistical analysis was performed by the analysis of variance followed by Tukey's HSD *post-hoc* test at 0.05 confidence level using JMP 17 program (SAS Institute Inc., Cary, NC, USA).

### Characterization of the solid residues after subcritical water treatment

**Field emission scanning electron microscopy.** Dry wood powder and residue (after SWE) were mounted on aluminum stubs using double-stick tape and coated with 5 nm platinum in a sputter coater (brand and country). Samples were examined using a Zeiss Merlin Field-emission Scanning Electron Microscope (FESEM, Carl Zeiss, Oberkochen, Germany) at an accelerated voltage of 5 kV. The width of macrofibrils was measured from SEM images using Image J software.<sup>36</sup> 25 random measurements were taken from the middle lamellae and inner secondary wall region on each image.

**Porosity analysis.** The surface area of the wood powder and residue was analyzed in triplicates with a single-point Tristar 3000 BET Brunauer–Emmett–Teller Analyzer (Micromeritics, Atlanta, GA, United States). The solid samples (100 mg) were subjected to degassing at 100 °C using a SmartPrep Degasser (Micromeritics) prior to the analysis to remove nonspecific adsorbents. The surface area was estimated from the multi-layered physical adsorption of nitrogen gas molecules according to the BET theory.<sup>37</sup>

**X-ray diffraction (XRD).** X-ray diffraction measurements were carried out in duplicates using a Panalytical X'pert Pro powder diffractometer (PANalytical, Netherlands) operating at 45 kV and 40 mA, with a Cu K $\alpha$  radiation anode. A radiation wavelength of 1.54 Å was used to record the diffraction patterns. The relative degree of crystallinity of the samples was obtained using the deconvolution method<sup>38</sup> in the range of 10–40°. The deconvolution of the intensity of the five crystal indexes 110, 1 $\text{N}$ 0, 120, 200, and 004 for crystalline cellulose index<sup>39</sup> and one broad peak at ~18° for amorphous cellulose was fitted by applying a Gaussian profile using OriginLab software.<sup>40</sup> Subsequently, the relative crystallinity (%RC) was calculated by dividing the integrated area of crystalline peaks ( $A_c$ ) with the total integrated area (amorphous ( $A_a$ ) and crystalline) as shown in eqn (1):

$$\% \text{ RC} = \frac{A_c}{(A_c + A_a)} \times 100 \quad (1)$$

**Fourier transform infrared spectroscopy (FTIR).** FTIR spectroscopy analysis was conducted in duplicates using a PerkinElmer Spectrum 100 instrument (Waltham, MA), equipped with a Golden Gate unit (single-reflection ATR). Sixteen consecutive scans were recorded and averaged between 4000 and 700 cm<sup>-1</sup> with a scanning step of 0.5 cm<sup>-1</sup> and a resolution of 4.0 cm<sup>-1</sup> for the spectra of the samples. The spectra were normalized to the maximum characteristic C–H peak intensity (1030 cm<sup>-1</sup>).

## Results and discussion

### Hemicellulose-first fractionation of aspen wood: validation in greenhouse and field conditions

Aspen has high industrial relevance as a promising biorefinery feedstock due to its fast growth and the desirable structural and chemical features of its woody biomass.<sup>41</sup> As a model plant for tree biotechnology, aspen trees are usually grown in controlled greenhouse conditions for approximately three months. However, trees grown in field conditions are exposed to both biotic and abiotic stresses leading to variation in phenotype and cell wall chemistry and are usually harvested after several growing seasons (Fig. 1A). Here we used the two types of hybrid aspen wood to test the applicability of SWE as an alternative pretreatment method that provides benefit of extracting its matrix cell wall polysaccharides for biorefinery applications. The sequential SWE process was implemented under buffered conditions on hybrid aspen wood without any pretreatment for delignification to yield maximum hemicellulose population with minimum deacetylation and autohydrolysis. The present study aimed to evaluate the efficiency of a hemicellulose-first hydrothermal process using SWE to promote saccharification of the biomass, compared to the traditional acid pretreatment (Fig. 1B).<sup>27</sup> This hemicellulose-first approach has the benefit to obtain a polymeric population of hemicelluloses that could be exploited in structural applications, as opposed to the degradative effect of acidic treatments. Aspen hemicelluloses include acetylated glucuronoxylan as the main component, with minor content of acetylated glucomannan (Fig. 1C).

Since growth conditions and growth duration are expected to influence the chemical composition of the lignocellulosic plant cell wall material, the SWE process and saccharification efficiency were validated in industrially relevant aspen wood grown in both greenhouse and field conditions. The cell wall chemistry analysis of both starting materials (Tables 1 and 2), reveals that aspen wood from the field has relatively higher lignin content, lower syringyl to guaiacyl (S/G) ratio, lower pectin and mannan content compared to that of greenhouse grown aspen (statistically significant at  $P \leq 0.05$ , ESI Table S3†). These differences between greenhouse and field grown trees can be attributed to changes in the wood cell wall structure and composition during wood juvenility-maturity transition<sup>42,43</sup> and to differences in stress exposure.<sup>44</sup> A similar higher guaiacyl (G) lignin content and lower S/G ratio in the field grown trees compared to greenhouse grown trees were reported previously.<sup>20</sup>

### Subcritical water extraction of aspen wood: mass balances, composition, and molar mass

The sequential subcritical water extraction process was evaluated for aspen wood grown in greenhouse and field conditions (Tables 1 and 2, respectively), based on the yields, composition and average molar mass of the sequential extracts (A1–A4) and the residue (R). Complete mass balances show that between 11–12% of the total solids were extracted. The monosaccharide



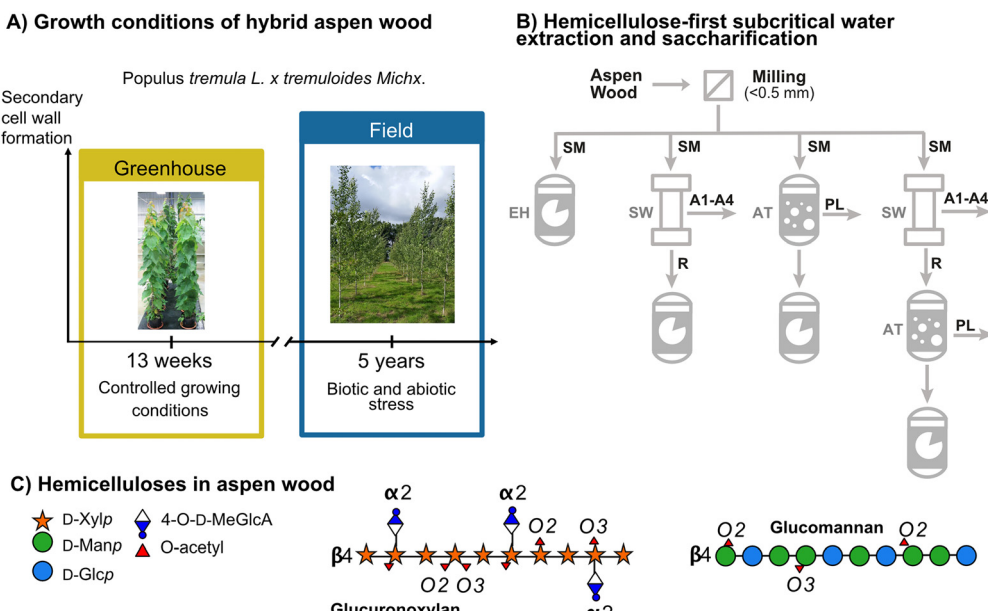


**Fig. 1** Hemicellulose-first processing prior to enzymatic saccharification of hybrid aspen grown in greenhouse and field conditions. (A) Comparison of hybrid aspen grown under greenhouse (G) and field (F) conditions. (B) Subcritical water extraction (SW) of hemicelluloses from aspen wood. Comparison to the untreated starting material (SM) and to conventional acid pretreatment (AT) prior to enzymatic saccharification (EH). (C) Molecular structures of the main hemicelluloses in hybrid aspen. Acetylated glucuronoxylan consists of a backbone of  $\beta$ -(1  $\rightarrow$  4)-xylose (Xyl) units decorated with  $\alpha$ -(1  $\rightarrow$  2)-4-O-methyl glucuronic acid (mGlcA) units and acetylated in the O-2 and/or O-3 positions. Acetylated glucomannan consists of a backbone of  $\beta$ -(1  $\rightarrow$  4)-mannose (Man) and  $\beta$ -(1  $\rightarrow$  4)-glucose (Glc) units decorated with acetylations in the O-2 and/or O-3 positions.

**Table 1** Mass balances and composition of the different fractions from greenhouse grown aspen

	SM	A1	A2	A3	A4	$\Sigma A$	R
Extraction time (min)	n.a	10	20	30	60	120	n.a
Total yield <sup>a</sup> (%)	100.0	2.9	2.2	2.7	3.3	11.1	88.9
Xylan yield <sup>b</sup> (%)	100.0	2.5	4.4	7.7	9.8	24.5	68.0
Lignin yield <sup>b</sup> (%)	100.0	2.1	1.7	2.0	2.4	8.3	27.7
Carbohydrate content <sup>b</sup> (mg/g)	647.0	706.5	670.8	773.7	791.1	679.7	
Cellulose <sup>b</sup> (%)	61.4	n.d.	n.d.	n.d.	n.d.	74.7	
Xylan <sup>b</sup> (%)	31.4	32.8	72.2	88.0	92.0	21.5	
Mannan <sup>b</sup> (%)	3.9	16.7	6.8	2.1	0.7	2.9	
Pectin <sup>b</sup> (%)	3.3	50.5	21.0	9.9	7.3	0.9	
MeGlcA : Xyl <sup>b</sup>	n.d.	0.32	0.18	0.20	0.21	n.d.	
Starch content <sup>c</sup>	0.16	0.4	0.2	0.2	0.2		
Lignin content <sup>d</sup> (ABL) (mg/g)	258.4	234.8	248.8	231.8	231.2	229.4	
Lignin content <sup>e</sup> (PyGCMS)(%)	34.9	20.0	17.2	16.3	13.2		
Guaiacyl <sup>e</sup> (%)	8.6	3.8	4.3	2.8	2.0		
Syringyl <sup>e</sup> (%)	25.4	12.1	7.8	10.6	8.9		
p-Hydroxyphenyl <sup>e</sup> (%)	0.8	3.9	5.0	2.8	2.2		
Phenolics <sup>e</sup> (%)	0.05	0.2	0.1	0.1	0.0		
S/G <sup>e</sup>	3.0	3.2	1.8	3.9	4.5		
C/L <sup>e</sup>	1.7	3.9	4.7	5.0	6.4		
Acetyl content <sup>f</sup> (%)	2.5	4.9	6.1	2.9	n.a		
$M_n$ (kDa) <sup>g</sup>	2.3	3.2	4.2	3.7	n.a		
$M_w$ (kDa) <sup>g</sup>	12.4	12.7	12.9	9.3	n.a		

<sup>a</sup> Yields determined gravimetrically and referred to the starting aspen wood chips. <sup>b</sup> Determined from the complete monosaccharide composition (ESI Table S1†). <sup>c</sup> Determined by starch gelatinization and enzymatic degradation. <sup>d</sup> Determined from acetyl bromide lignin. <sup>e</sup> Determined from pyrolysis GC-MS. <sup>f</sup> Determined after saponification and HPLC-UV analysis. <sup>g</sup> Determined by SEC-DRI. A1-A4 indicate sequential extraction time: A1 (10 min), A2 (20 min), A3 (30 min), A4 (60 min). n.a. not applicable; n.d. not detected; S/G Syringyl-Guaiacyl ratio; C/L Carbohydrate-Lignin ratio.

composition of the sequential extracts confirms that non-cellulosic polysaccharides (pectins, glucomannan and mainly glucuronoxylan) were primarily extracted in the SWE process,

while cellulose was mainly left in the residue (Fig. 2A). The A1 and A2 extracts were rich in pectin, as revealed by the high content of diagnostic rhamnose (Rha), arabinose (Ara) galac-



Table 2 Mass balances and composition of the different fractions from field grown aspen

	SM	A1	A2	A3	A4	ΣA	R
Extraction time (min)	n.a	10	20	30	60	120	n.a
Total yield <sup>a</sup> (%)	100.0	2.2	2.1	3.5	4.1	11.9	88.1
Xylan yield <sup>b</sup> (%)	100.0	1.8	4.7	10.0	13.1	29.6	67.9
Lignin yield <sup>b</sup> (%)	100.0	1.9	1.9	2.9	3.5	10.2	27.3
Carbohydrate content <sup>b</sup> (mg g <sup>-1</sup> )	673.5	629.9	719.3	826.0	921.7	n.a.	691.4
Cellulose <sup>b</sup> (%)	61.7	n.d.	n.d.	n.d.	n.d.		75.5
Xylan <sup>b</sup> (%)	32.5	38.1	80.6	91.5	93.2		21.4
Mannan <sup>b</sup> (%)	3.1	21.2	5.1	1.4	0.8		2.2
Pectin <sup>b</sup> (%)	2.7	40.6	14.4	7.2	6.0		0.9
MeGlcA : Xyl <sup>b</sup>	n.d.	0.31	0.20	0.21	0.24	n.d.	
Starch content <sup>c</sup>	0.45	6.6	1.6	0.5	0.2		
Lignin content <sup>d</sup> (ABL) (mg g <sup>-1</sup> )	285.7	258.4	263.4	242.2	249.0		242.6
Lignin content <sup>e</sup> (PyGCMS) (%)	36.9	29.2	19.8	14.5	15.3		
Guaiacyl <sup>e</sup> (%)	10.4	6.9	3.1	1.8	1.8		
Syringyl <sup>e</sup> (%)	23.2	17.4	14.0	10.7	11.8		
p-Hydroxyphenyl <sup>e</sup> (%)	3.2	4.9	2.6	1.9	1.6		
Phenolics <sup>e</sup> (%)	0.04	0.1	0.1	0.1	0.0		
S/G <sup>e</sup>	2.2	2.5	4.6	5.8	6.7		
C/L <sup>e</sup>	1.8	2.4	4.0	5.8	5.4		
Acetyl content <sup>f</sup> (%)		2.8	4.6	6.8	2.9		
<i>M<sub>n</sub></i> <sup>g</sup> (kDa)		1.7	3.2	4.6	3.3		
<i>M<sub>w</sub></i> <sup>g</sup> (kDa)		7.8	12.1	13.3	7.9		

<sup>a</sup>Yields determined gravimetrically and referred to the starting aspen wood chips. <sup>b</sup>Determined from the complete monosaccharide composition (ESI Table S2†). <sup>c</sup>Determined by starch gelatinization and enzymatic degradation. <sup>d</sup>Determined from acetyl bromide lignin. <sup>e</sup>Determined from pyrolysis GC-MS. <sup>f</sup>Determined after saponification and HPLC-UV analysis. <sup>g</sup>Determined by SEC-DRI. A1–A4 indicate sequential extraction time: A1 (10 min), A2 (20 min), A3 (30 min), A4 (60 min). n.a. not applicable; n.d. not detected; S/G Syringyl–Guaiacyl ratio; C/L Carbohydrate–Lignin ratio

tose (Gal) and galacturonic acid (GalA) monosaccharides. As expected, these extracts from the greenhouse grown trees showed a higher pectin content compared to field grown trees ( $P \leq 0.05$ , *t*-test). The higher pectin content may be related to the reduced amount of the secondary wall relative to the compound middle lamella in the more juvenile wood of greenhouse grown trees.<sup>43,45–48</sup> A relatively high glucan content was observed in the 10 min extracts (A1) for both greenhouse and field samples, which could be attributed to residual starch, primary cell wall xyloglucan, and/or callose. Interestingly, the glucan content in the field extract at 10 min was more than double than for greenhouse ( $P \leq 0.05$ , *t*-test), which could be related to the higher occurrence of starch (Tables 1 and 2,  $P \leq 0.05$ , *t*-test) and probably also callose in the field due to overwintering and higher stress levels experienced by the trees. Indeed, both starch and callose are known to accumulate in responses to biotic and abiotic stresses.<sup>44</sup> Mannan represents a minor part of hemicellulose composition in hardwoods.<sup>49</sup> Aspen glucomannan is reported to have a mannose to glucose ratio of 1.3–2 : 1 and are attached with O-acetyl groups at C2 and C3 of mannosyl residues.<sup>50</sup> The SWE process showed a higher mannan population in the A1 extract compared with subsequent extracts suggesting preferential extraction of mannan along with pectic components during short extraction time (10 min). The high extractability of the mannan could be related to its spatial distribution in primary and secondary cell walls, and/or its interaction with cellulose and other cell wall components.<sup>51,52</sup>

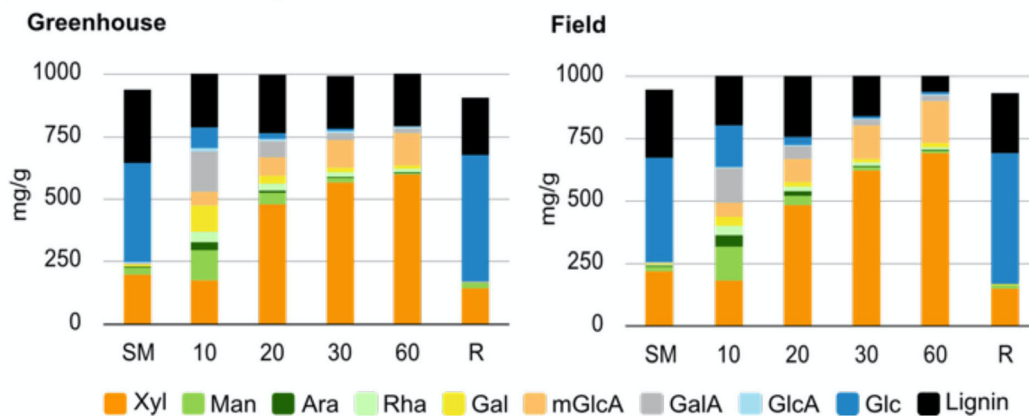
Xylan represents approximately between 31–32% of the aspen wood dry weight. About 25–30% of this xylan could be

extracted in polymeric form with during the 2-hour SWE process (Tables 1, 2 and Fig. 2). However, 68% of the xylan in the aspen wood could not be fractionated and was left in the residue, whereas 3–7.5% of the total solid were lost during dialysis corresponding to low molar mass compounds. These yields are comparable to a 5-hour extraction from birch wood.<sup>2</sup> The total xylan yield in the extracts was relatively higher in field grown aspen compared to that of greenhouse aspen which probably reflects the higher relative content of secondary walls in more mature wood from the field.<sup>45</sup> As expected, the purity of xylan increased with extraction time, reaching about 93% of the carbohydrate composition for the A3 and A4 extracts. The molecular xylan structure in aspen was assessed by the glucuronosyl (MeGlcA) and acetyl (Ac) substitution contents and patterns. The acetyl content increased gradually during extraction from A1 to A3 while it decreased significantly in A4, suggesting deacetylation of xylan during longer extraction periods. On the other hand, the MeGlcA : Xyl ratio gradually increased from A2 to A4 (Tables 1 and 2) with a significant difference between A3–A4 ( $P \leq 0.05$ , ESI Table S4†), which indicate tighter glucuronation for the recalcitrant xylan fractions, as previously reported for birchwood.<sup>2</sup>

The molar mass profiles of the sequential SWE extracts (Fig. 2B) show similar trends between the greenhouse and the field starting materials. A1 extracts showed multimodal distributions, including a population of larger molar mass polymers (between  $10^5$ – $10^6$  Da) that could be attributed to starch,<sup>2</sup> and a population of small molar mass compounds (500 Da) that might be assigned to extractives. The xylan-rich extracts (A2–



## A) Monosaccharide composition



## B) Molar mass distributions

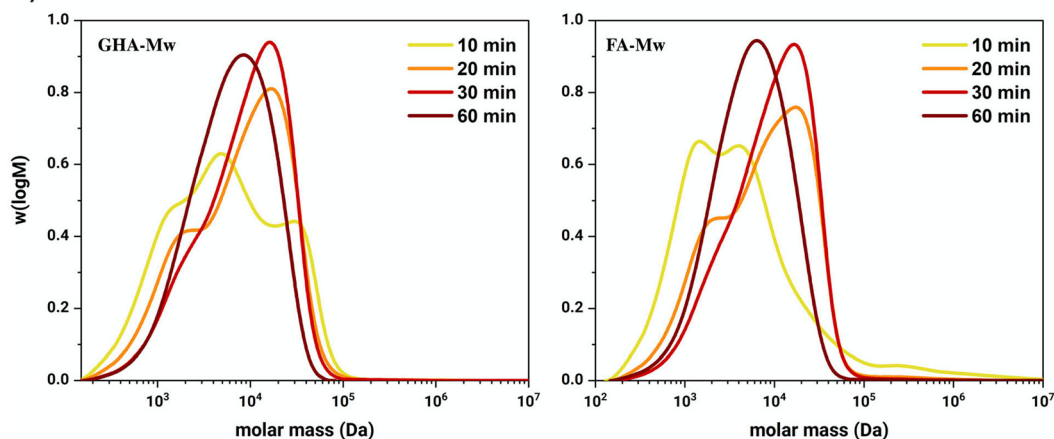


**Fig. 2** Composition of extracts obtained by SWE. (A) Monosaccharide composition of starting material (SM), SW extracts at 10, 20, 30 and 60 min, and residue (R) from greenhouse and field samples. (B) Molar mass distributions of field (F) and greenhouse (G) SW extracts.

A4) show that the extracted compounds conserved their polymeric structure between  $10^4$  to  $10^5$  Da corresponding to hardwood xylan.<sup>2</sup> The A2 extracts showed bimodal molar mass distributions, with a main population above  $10^4$  Da and a minor shoulder between  $10^3$ – $10^4$  Da. These two distinct populations become more evident by comparing the signals from the refractive index (DRI) and ultraviolet (UV) detectors (ESI Fig. S1†). The high molar mass regions in the A2 extracts exhibited relatively weak UV signals that correlate with lower lignin content, whereas the low molar mass populations exhibited a prominent UV peak that indicates a larger aromatic abundance that could be assigned to lignin-carbohydrate complexes. This contrasts with previous observations on alkali-extracted xylan that can effectively remove the lignin moieties attached to the hemicelluloses.<sup>53</sup> Finally, longer extraction times result in a shift of the molar mass distributions to lower values as evidenced in the A4 extracts, confirming the occurrence of hydrolytic events during longer exposure times. Indeed, Martínez-Abad *et al.* (2018)<sup>2</sup> reported that the extraction in subcritical conditions is largely governed by mass transfer and diffusion kinetics of matrix cell wall polymers to

the liquid phase, and that higher temperature and controlled mild acidic pH provide a compromise between molar mass, yield and purity. This explains the similar composition and molar mass in extracts A2–A3 and the drastic decrease in molar mass of A4 extract due to hydrolytic depolymerization (Fig. 2B).

The cell wall compositional analysis by pyrolysis GC-MS revealed that the lignin content and monolignol yield for G, S and H units decreased in successive extracts whereas the S/G ratio increased (Tables 1, 2 and  $P \leq 0.05$ , ESI Table S5†). This suggests a high recalcitrance of guaiacyl units to water extraction process. The field grown trees showed higher S/G ratio in A2–A4 extracts than greenhouse grown trees, which is mainly contributed by their higher syringyl monolignol content. On the other hand, the carbohydrate to lignin (C/L) ratio increased over the time due to the high hemicellulose extraction yield. The different extractability of monolignol components between greenhouse and field grown aspen also suggests the possible change in the dynamics of molecular interaction between cell wall polymers during xylem juvenility-maturity transition.



## The effect of SWE treatment on the morphology of the wood residue

The effect of the hydrothermal conditions on the morphology and ultrastructure of the cellulose-rich insoluble fractions after subcritical water treatment were evaluated by Fourier transform infrared spectroscopy (FTIR), X-ray diffraction (XRD) and scanning electron microscopy. SEM analysis of starting material showed the occurrence of cellulose fibrils embedded in matrix polymers, giving a smooth appearance to the inner surface layer (S3 layer) (Fig. 3A). Macrofibrils were readily observed in the compound middle lamellae (CML) region often stretched and fractured during the milling process (Fig. 3A). The effect of growth conditions on wood macrofibril dimensions was evaluated. The field grown trees showed larger macrofibril width compared to greenhouse grown trees ( $P \leq 0.05$ , Table 3 and ESI Table S6†). In *Pinus* and *Populus* wood, macrofibril diameter is linearly related to lignin concentration.<sup>54</sup> Lignin is assumed to infiltrate the cellulose macrofibril aggregates during lignification resulting in swelling of the aggregates.<sup>55</sup> Moreover, the macrofibril size also depends on xylan content.<sup>56</sup> More mature wood of field grown aspen might have higher lignin concentration and higher xylan content than that of greenhouse grown plants. SEM analysis was also used to evaluate the effect of SWE process on the structure and dimensions of cellulose macrofibrils in the residue. The residue from the greenhouse grown trees after SWE extraction showed loosening of macrofibrils in the form of a web-like organization (Fig. 3A). The field grown trees also showed swelling of the secondary wall and macrofibril loosening. Previous studies have reported that cellulose aggregation after pulping processes is related to the residual hemicellulose content, where cellulose fibrils aggregate and the macrofibril size increases with decreasing hemicelluloses content.<sup>57,58</sup> However, in the present study, the width of macrofibrils showed a slight reduction between aspen wood and residue after hydrothermal treatment. This suggests that the lignin infiltrated within the macrofibril organization somehow preserves its dimension after hydrothermal treatment and prevents macrofibril aggregation, in contrast to cellulose fibrils observed in wood pulps that had been subjected to delignification processes. The changes in the cell wall architecture during SWE were further evident from the BET analysis of lignocellulose porosity. A significant increase in surface area was noticed in the residue compared to that of starting material ( $P \leq 0.05$ , ESI Table S7† and Table 3), which is related to the preferential extraction of acetylated GX during SWE. The increase in porosity was twofold higher in greenhouse samples compared to field samples ( $P \leq 0.05$ , ESI Table S7†). This could be attributed to the more juvenile and less compact wood cell wall structure in greenhouse samples compared to the field ones.<sup>59</sup>

The FTIR spectra from the starting aspen wood showed the chemical features attributed to the specific cell wall components (Fig. 3B), including C-H stretching at 2800–3000  $\text{cm}^{-1}$ , O-H stretching at 3300–3600  $\text{cm}^{-1}$ , and

several peaks in the region between 700 and 1750  $\text{cm}^{-1}$  that have contributions from both carbohydrates and lignin. The evidence of the preferential extraction of acetylated glucuronoxylan was evident from a decrease in the intensities of 1735 (C=O ester) and 1230  $\text{cm}^{-1}$  (–C–O– stretching band) in the FTIR spectra of the SWE residues, which are assigned for the ester stretching of the acylated hemicelluloses.<sup>38,39</sup> On the other hand, the increase at 1590  $\text{cm}^{-1}$  (lignin skeletal vibrations from the C–C,<sup>38,39</sup> 1080  $\text{cm}^{-1}$  and 1055  $\text{cm}^{-1}$  (C–O and C–O–C of cellulose<sup>38,39</sup> further confirmed the relative enrichment of cellulose and lignin in the SWE residue (R). Moreover, ATR-FTIR was used to investigate the crystallinity and hydrogen bonding characteristics of the cellulose microfibrils.<sup>60</sup> The Lateral order index (LOI,  $\alpha_{1418/894}$ ), hydrogen bond intensity (HBI,  $\alpha_{3336/1336}$ ), and total crystallinity intensity (TCI,  $\alpha_{1364/2892}$ ), based on the ratio of absorbance bands at specific wavenumbers, were used to interpret qualitative changes in cellulose crystallinity.<sup>60</sup> An increase of LOI and TCI were observed in the residues from SWE treatment from the field and the greenhouse compared to the starting material (Table 3), which suggest an increase in overall crystallinity of the residue due to selective removal of amorphous hemicellulose material.

X-ray diffraction (XRD) was performed on the original solid material and after SWE treatment to obtain a deeper understanding of the crystalline arrangement of the aspen biomass (Fig. 3c). The XRD patterns from all the samples exhibit the typical crystalline peaks of cellulose I at 15–16° (100) and 22° (200), as previously reported<sup>61–63</sup> The crystal peaks were investigated with the deconvolution method, in order to obtain the relative crystallinity of the different samples.<sup>64</sup> The XRD results verified the preliminary assessment from FTIR, indicating that the residue after SWE have higher crystallinity after the extraction of hemicelluloses and result in more pronounced XRD crystalline peaks (Table 3 and ESI Table S8†). We have qualitatively normalized the overall degree of crystallinity to the cellulose content in the starting materials and residues after SWE, to assess whether the hydrothermal process had an impact on the specific crystallinity of the cellulose components. The comparison suggests that the hemicelluloses in the starting materials contribute to their overall crystallinity, and that the SWE treatment somehow influences the organization of the cellulose components reducing the specific crystallinity of the cellulose microfibrils. This different organization of the cellulose components will have an influence on the recalcitrance and saccharification potential of the aspen biomass, as will be discussed later.

## Subcritical water enhances the saccharification potential of aspen wood

To understand the influence of hydrothermal extraction of matrix polymers on reducing lignocellulose recalcitrance of aspen wood, we evaluated the effect of SWE on enzymatic saccharification of the SW residue in comparison with the untreated starting material and conventional acid pretreatment as a reference. The effect of applying the conventional



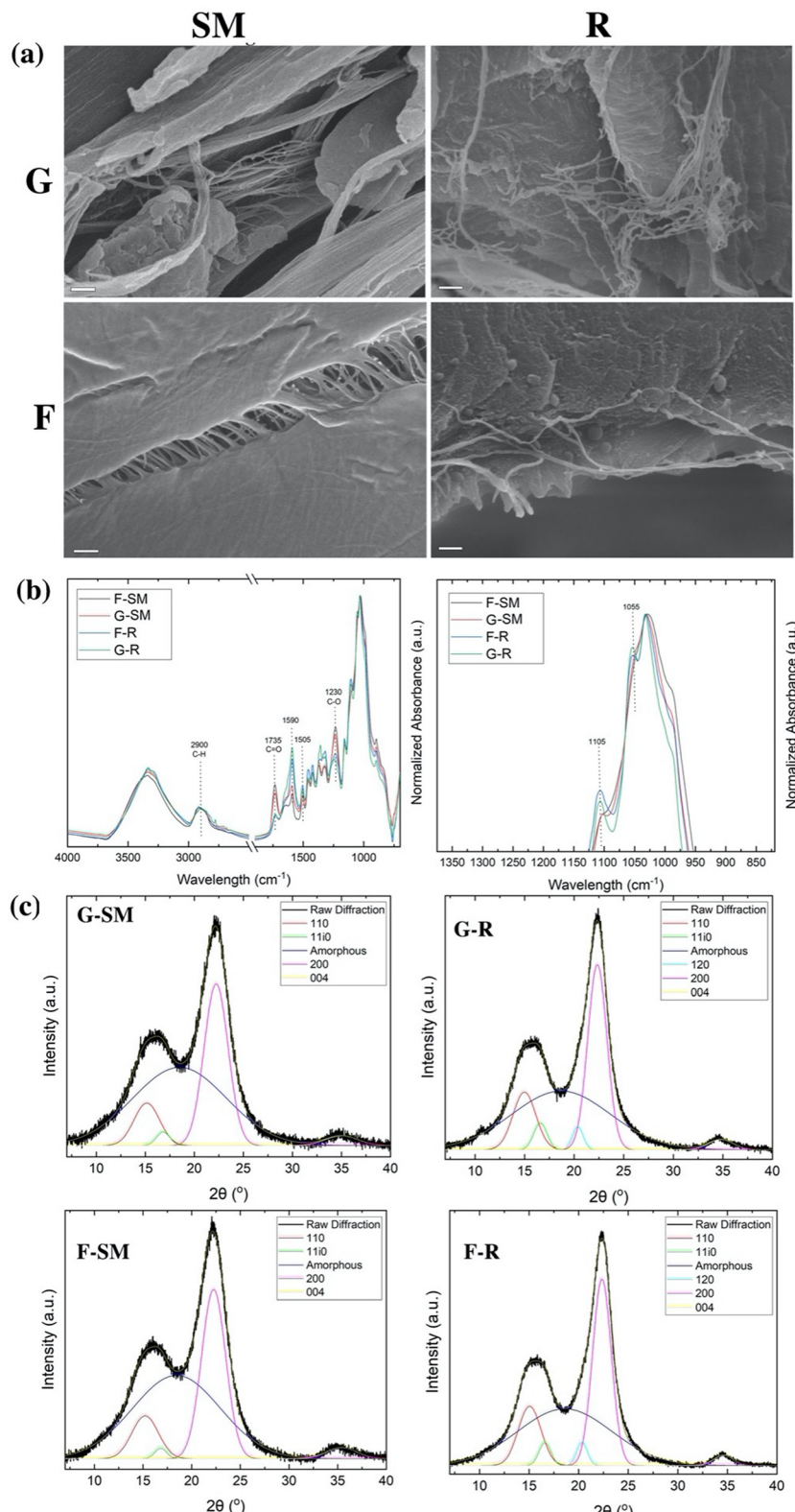


**Fig. 3** Structural characteristics of starting material (SM) and residue (R) of aspen wood grown in Greenhouse (G) and field (F) conditions. (a) FTIR spectra, (b) X-ray diffraction pattern and (c) Scanning electron microscopy (SEM), SEM scale bar = 200 nm.



**Table 3** Relative crystallinity index, normalized crystallinity, macrofibril width and BET-Surface area of starting material (SM) and SWE residue (R) of wood from aspen trees grown in green house (G) and field (F) conditions

	G-SM	F-SM	G-R	F-R
Macrofibril width (nm)	14 ± 0.6	17.1 ± 1.0	12.0 ± 0.4	15.0 ± 0.5
BET surface area (m <sup>2</sup> g <sup>-1</sup> )	1.40 ± 0.04	1.86 ± 0.17	3.08 ± 0.20**	2.2 ± 0.17*
Lateral order index	0.80 ± 0.08	0.77 ± 0.10	0.91 ± 0.10	0.91 ± 0.20
Hydrogen bond intensity	0.99 ± 0.2	0.95 ± 0.3	0.91 ± 0.2	0.91 ± 0.2
Total crystallinity intensity	1.63 ± 0.01	1.56 ± 0.03	1.76 ± 0.02	1.58 ± 0.06
Degree of crystallinity (%)	42.8 ± 0.11	43.7 ± 0.05	48.6 ± 0.1*	50.2 ± 0.6*

Mean ± STDev of 3 technical replicates. Asterisk (\*) indicates statistically significant difference for significant difference between SWE treated and SWE untreated samples of same growth condition determined by Student's *t*-test  $P \leq 5\%$  (\*);  $P \leq 1\%$  (\*\*). Indices calculated at TCI =  $\alpha 1364/2892$ ; LOI =  $\alpha 1418/893$ ; HBI =  $\alpha 3338/1334$ .

acid treatment on the subcritical water residue prior to saccharification was also evaluated. In both greenhouse and field grown aspen, subcritical water extraction clearly improved the saccharification efficiency of wood, as evidenced by the significantly higher glucose production rate (GPR) compared to the control sample without any pretreatment (Fig. 4A). Moreover, SWE treatment increased fourfold the total glucose and xylose yields after saccharification of the residue, compared to those of starting material without any pretreatment (Fig. 4B and ESI Tables S9, S10†). This can be correlated with the higher porosity, lower inherent crystallinity of the cellulose, and the increased fibrillation caused by the SWE treatment compared to the starting material, as revealed by the XRD, SEM and BET results (Fig. 3). The removal of hemicelluloses attached to cellulose microfibrils, the subsequent reduced acetyl content, and the increase in surface area in the residues caused by SWE seems to enhance enzymatic accessibility towards cellulose, leading to efficient conversion of glucose during saccharification without pretreatment. Indeed, a lower surface area of wood starting material compared to the SWE residue due to hemicellulose coating the cellulose surfaces and the presence of lignin, along with the high crystallinity of cellulose are major limiting factors for effective access of hydrolytic

enzymes to cellulose during saccharification process.<sup>14,15</sup> Interestingly, the starting materials from greenhouse grown trees showed relatively higher glucose production rate compared to that of field grown trees with and without SWE process (Fig. 4A and ESI Table S11†), suggesting that enzyme accessibility might differ in both cases due to composition (*i.e.* lower lignin content) and wood cell ultrastructure (*i.e.* smaller microfibril diameter and degree of crystallinity).<sup>23,65</sup>

Comparing the conventional acid pretreatment (AP) with the subcritical water (SW) process, interesting conclusions can be drawn. The acid pretreatment causes a significant increase in the glucose production rate compared to the subcritical water process, related to the higher glucose content released in the acid hydrolysate (PL) and the subsequent enzymatic hydrolysis (EH). However, comparing the total sugars, the SW process enables similar release compared to the acid pretreatment, which can be attributed to the enzymatic release of xylose from the residual xylan that could not be extracted in the SW process. Indeed, most of the xylose is released during the acid pretreatment in the liquid phase (PL) and therefore is not available in the following enzymatic saccharification step. The fact that the xylose released in the saccharification step after SW extraction is similar to the xylose released in the acid

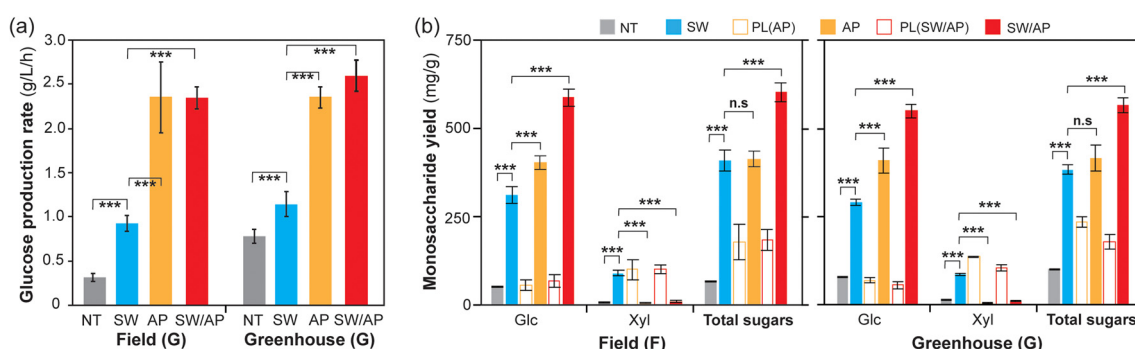


**Fig. 4** Enzymatic saccharification of aspen lignocellulose biomass from greenhouse (G) and field (F) under four different treatment conditions as depicted in Fig. 1B: untreated starting material (NT), subcritical water (SW), acid pretreatment (AP) and subcritical water followed by acid pretreatment (SW/AP). (a) Glucose production rate (g L<sup>-1</sup> h<sup>-1</sup>). (b) Monosaccharide yield for glucose (Glc), xylose (Xyl) and total sugars from the enzymatic saccharification. The complete released monosaccharides are presented in ESI Tables S9 and S10† for field and greenhouse aspen, respectively. PL refers to the liquid hydrolysate obtained after acid pretreatment (AP) containing fermentable sugars. The asterisks (\*) indicate statistically significant differences between the enzymatic saccharification of the SW residue compared to the other treatments determined by Student's *t*-test (ESI Tables S12 and S13†):  $P \leq 5\%$  (\*);  $P \leq 1\%$  (\*\*);  $P \leq 0.1\%$  (\*\*\*)<sup>†</sup>. n.s: not statistically significant.



**Table 4** Total mass balance of carbohydrates (as polysaccharides or monosaccharides) and xylan/xylose balance released during the combined subcritical water extraction and enzymatic saccharification process

	Field (F)				Greenhouse (G)			
	NT	SW	AP	SW/AP	NT	SW	AP	SW/AP
SWE polysaccharides (%)	—	11.9	—	11.9	—	11.1	—	11.1
Total sugars PL (%)	—	—	17.8	18.6	—	—	23.5	17.8
Total sugars EH (%)	6.8	40.9	41.2	60.3	10.1	38.4	41.7	56.7
Total mass balance (%)	6.8	52.8	59.0	90.8	10.1	49.5	65.2	85.6
SWE xylan (%)	—	29.6	—	29.6	—	24.5	—	24.5
Total xylose PL (%)	—	—	30.9	31.2	—	—	43.5	33.0
Total xylose EH (%)	3.1	28.1	1.7	3.2	4.5	27.5	1.5	3.4
Xylan/xylose balance (%)	3.1	57.7	32.5	64.0	4.5	52.0	45.0	60.9

SW (subcritical water extraction); PL (hydrolysate acid pre-treatment); EH (hydrolysate enzymatic saccharification).

hydrolysate (PL) suggests the occurrence of degradation, as it will be confirmed later in the full mass balances. Finally, performing an acid pretreatment step after subcritical water significantly increases the release of glucose release and overall total sugars compared to both the subcritical water and the acid pretreatment performed alone.

Mass balances were performed on the total polysaccharides and the xylan/xylose for the four different treatments evaluated in this study (Table 4). The acid pretreatment still offers higher total yields that the subcritical water process, all in the form of hydrolysed monosaccharides, although the SW process is able to preserve the polymeric structure of the xylan in the extraction step prior to saccharification. Interestingly, the combination of SW and AP can reach almost 85–90% conversion of the initial polysaccharides into fermentable sugars. When comparing the xylan yields alone, the SW process clearly outperforms the traditional acid hydrolysis, which could be due to the degradation of the xylose into furan derivatives caused by the acid conditions. All in all, our results suggests that the hemicellulose first extraction by SWE process is an efficient process to reduce the requirement of acid pretreatment during the conversion of wood biomass for biorefinery applications, by on one hand preserving the polymeric structure of the extracted xylan that could be used for valuable material applications (*i.e.* as barrier or biomedical matrices) and enabling the subsequent conversion of the residual biomass into fermentable sugars by enzymatic saccharification.

## Conclusions

The present study demonstrates the efficacy of subcritical water extraction in the fractionation of non-cellulosic polysaccharides from aspen wood and validates the process for aspen trees grown in controlled greenhouse and real field conditions. Greenhouse conditions enable the control of the different environmental parameters during aspen growth, whereas field growth represent a more realistic case close to industrial application, where biotic and abiotic conditions also play a role

during lignocellulose development. For both conditions, subcritical water induces morphological changes in the residual lignocellulosic biomass, reducing its native recalcitrance to enzymatic hydrolysis and favoring its subsequent saccharification. The sequential SWE process of aspen wood extracts pectic polysaccharides at short times (below 10 min), whereas longer extraction times (between 2–60 min) promote the extraction of hemicelluloses in polymeric form, mainly acetylated glucuronoxylan. Longer extraction times (>60 min) induce deacetylation of the isolated xylan and a reduction in the molecular weight, caused by hydrolytic processes under the subcritical water conditions. When comparing aspen grown in greenhouse and field conditions, the SWE shows very similar behaviour, with only slight differences in the pectin and glucan content in the short time extracts, which could be assigned to the different stages of wood development between growth conditions and the response to environmental stress (abiotic and biotic) in the field trees. The fractionation of cell wall matrix polysaccharides by SWE process induces structural changes in the lignocellulosic biomass, including higher porosity and lower fibril dimensions. These structural and chemical changes lead to significantly higher yields of glucose and xylan in enzymatic saccharification compared to yields from not treated aspen wood chips. We hypothesize that the saccharification potential was enhanced by the increased accessibility of hydrolytic enzymes into the residual biomass, caused by the removal of acetylated glucuronoxylan and associated changes in the surface morphology and cell wall porosity. Compared to the traditional acid pretreatment that hydrolyses the hemicellulose components, SW offers comparable yields of fermentable sugars with the advantage of providing an initial hemicellulose fraction with preserved macromolecular structure, which could be used as a biopolymeric matrix in barrier and structural applications. This study highlights the potential of SWE to extract native hemicellulose, and also as a green pretreatment strategy to reduce biomass recalcitrance contributed by non-cellulosic polysaccharides, thereby decreasing the requirement of acid pre-treatments during biochemical conversion of aspen wood.



## Conflicts of interest

Francisco Vilaplana reports a relationship with Oatly AB that includes employment.

## Acknowledgements

The authors acknowledge the financial support from the Swedish Research Council (Project Grant 2020-04720) and the Knut and Alice Wallenberg Foundation (KAW) to the Wallenberg Wood Science Centre. F. V. and P. S. acknowledge the BioUPGRADE project for the financial contribution. This project has received funding from the European Union's Horizon 2020 research and innovation programme under grant agreement no. 964764. The content presented in this document represents the views of the authors, and the Commission is not responsible for any use that may be made of the information it contains. The authors are thankful for the access to the facilities and the technical assistance of the Umeå Centre for Electron Microscopy – National Microscopy Infrastructure (UCEM-NMI) and Bioanalytical Platform, Umeå Plant Science Centre (UPSC), Umeå for access to Pyrolysis-GCMS analysis.

## References

- Y. M. Bar-On, R. Phillips and R. Milo, *Proc. Natl. Acad. Sci. U. S. A.*, 2018, **115**, 6506–6511.
- A. Martínez-Abad, N. Giummarella, M. Lawoko and F. Vilaplana, *Green Chem.*, 2018, **20**, 2534–2546.
- X. Yang, D. Liu, H. Lu, D. J. Weston, J.-G. Chen, W. Muchero, S. Martin, Y. Liu, M. M. Hassan, G. Yuan, U. C. Kalluri, T. J. Tschaplinski, J. C. Mitchell, S. D. Wullschleger and G. A. Tuskan, *BioDesign Res.*, 2021, 9798714.
- D. Keegan, B. Kretschmer, B. Elbersen and C. Panoutsou, *Biofuels, Bioprod. Bioref.*, 2013, **7**, 193–206.
- B. Thomas, M. C. Raj, B. K. Athira, H. M. Rubiyah, J. Joy, A. Moores, G. L. Drisko and C. Sanchez, *Chem. Rev.*, 2018, **118**, 11575–11625.
- E. Kontturi, P. Laaksonen, M. B. Linder, A. H. Nonappa, A. H. Gröschel, O. J. Rojas and O. Ikkala, *Adv. Mater.*, 2018, **30**, 1703779.
- T. Li, C. Chen, A. H. Brozena, J. Y. Zhu, L. Xu, C. Driemeier, J. Dai, O. J. Rojas, A. Isogai, L. Wågberg and L. Hu, *Nature*, 2021, **590**, 47–56.
- S. Sen, S. Patil and D. S. Argyropoulos, *Green Chem.*, 2015, **17**, 1077–1087.
- W. J. Liu, H. Jiang and H. Q. Yu, *Green Chem.*, 2015, **17**, 4888–4907.
- A. J. Ragauskas, G. T. Beckham, M. J. Biddy, R. Chandra, F. Chen, M. F. Davis, B. H. Davison, R. A. Dixon, P. Gilna, M. Keller, P. Langan, A. K. Naskar, J. N. Saddler, T. J. Tschaplinski, G. A. Tuskan and C. E. Wyman, *Science*, 2014, **344**, 1246843.
- W. Zhao, B. Simmons, S. Singh, A. Ragauskas and G. Cheng, *Green Chem.*, 2016, **18**, 5693–5700.
- A. Duval and M. Lawoko, *React. Funct. Polym.*, 2014, **85**, 78–96.
- K. S. Mikkonen, *Green Chem.*, 2020, **22**, 1019–1037.
- M. C. McCann and N. C. Carpita, *J. Exp. Bot.*, 2015, **66**, 4109–4118.
- M. E. Himmel, S. Y. Ding, D. K. Johnson, W. S. Adney, M. R. Nimlos, J. W. Brady and T. D. Foust, *Science*, 2007, **315**, 804–807.
- P. A. Penttilä, A. Várnai, J. Pere, T. Tammelin, L. Salmén, M. Siika-aho, L. Viikari and R. Serimaa, *Bioresour. Technol.*, 2013, **129**, 135–141.
- E. Heinonen, G. Henriksson, M. E. Lindström, F. Vilaplana and J. Wohlert, *Carbohydr. Polym.*, 2022, **285**, 119221.
- J. Berglund, D. Mikkelsen, B. M. Flanagan, S. Dhital, S. Gaunitz, G. Henriksson, M. E. Lindström, G. E. Yakubov, M. J. Gidley and F. Vilaplana, *Nat. Commun.*, 2020, **11**, 4692.
- A. Martínez-Abad, A. Jiménez-Quero, J. Wohlert and F. Vilaplana, *Green Chem.*, 2020, **22**, 3956–3970.
- G. Gallina, E. R. Alfageme, P. Biasi and J. García-Serna, *Bioresour. Technol.*, 2018, **247**, 980–991.
- P. O. Kilpeläinen, S. S. Hautala, O. O. Byman, L. J. Tanner, R. I. Korpinen, M. K. J. Lillandt, A. V. Pranovich, V. H. Kitunen, S. M. Willför and H. S. Ilvesniemi, *Green Chem.*, 2014, **16**, 3186–3194.
- R. C. Rudjito, A. Jiménez-Quero, M. Hamzaoui, S. Kohnen and F. Vilaplana, *Green Chem.*, 2020, **22**, 8337–8352.
- S. Pramod, M. L. Gandla, M. Derba-Maceluch, L. J. Jönsson, E. J. Mellerowicz and S. Winestrand, *Front. Plant Sci.*, 2021, **12**, 704960.
- P. Sannigrahi, A. J. Ragauskas and G. A. Tuskan, *Biofuels, Bioprod. Bioref.*, 2010, **4**, 209–226.
- E. N. Donev, M. Derba-Maceluch, Z. Yassin, M. L. Gandla, P. Sivan, S. E. Heinonen, V. Kumar, G. Scheepers, F. Vilaplana, U. Johansson, M. Hertzberg, B. Sundberg, S. Winestrand, A. Hörnberg, B. Alriksson, L. J. Jönsson and E. J. Mellerowicz, *Plant Biotechnol. J.*, 2023, 1005–1021.
- M. L. Gandla, M. Derba-Maceluch, X. Liu, L. Gerber, E. R. Master, E. J. Mellerowicz and L. J. Jönsson, *Phytochemistry*, 2015, **112**, 210–220.
- Z. Wang, S. Winestrand, T. Gillgren and L. J. Jönsson, *Biomass Bioenergy*, 2018, **109**, 125–134.
- F. Bertaud, A. Sundberg and B. Holmbom, *Carbohydr. Polym.*, 2002, **48**, 319–324.
- L. S. McKee, H. Sunner, G. E. Anasontzis, G. Toriz, P. Gatenholm, V. Bulone, F. Vilaplana and L. Olsson, *Biotechnol. Biofuels*, 2016, **9**, 2.
- J. F. Saeman, W. E. Moore, R. L. Mitchell and M. A. Millett, *Tappi J.*, 1954, **37**, 336–343.
- C. E. Foster, T. M. Martin and M. Pauly, *J. Visualized Exp.*, 2010, **37**, 1745.



32 M. Stitt, R. M. C. Lilley, R. Gerhardt and H. W. Heldt, *Methods Enzymol.*, 1989, **174**, 518–552.

33 J. H. M. Hendriks, A. Kolbe, Y. Gibon, M. Stitt and P. Geigenberger, *Plant Physiol.*, 2003, **133**, 838–849.

34 A. M. Smith and S. C. Zeeman, *Nat. Protoc.*, 2006, **1**, 1342–1345.

35 L. Gerber, M. Eliasson, J. Trygg, T. Moritz and B. Sundberg, *J. Anal. Appl. Pyrolysis*, 2012, **95**, 95–100.

36 C. A. Schneider, W. S. Rasband and K. W. Eliceiri, *Nat. Methods*, 2012, **9**, 671–675.

37 S. Lowell and J. E. Shields, in *Powder Surface Area and Porosity*, ed. S. Lowell and J. E. Shields, Springer Netherlands, Dordrecht, 1991, pp. 14–29. DOI: [10.1007/978-94-015-7955-1\\_4](https://doi.org/10.1007/978-94-015-7955-1_4).

38 F. Nindiyasari, E. Griesshaber, T. Zimmermann, A. P. Manian, C. Randow, R. Zehbe, L. Fernandez-Diaz, A. Ziegler, C. Fleck and W. W. Schmahl, *J. Compos. Mater.*, 2016, **50**, 657–672.

39 M. Fasoli, R. Dell'Anna, S. Dal Santo, R. Balestrini, A. Sanson, M. Pezzotti, F. Monti and S. Zenoni, *Plant Cell Physiol.*, 2016, **57**, 1332–1349.

40 S. I. Andersen, J. O. Jensen and J. G. Speight, *Energy Fuels*, 2005, **19**, 2371–2377.

41 C. Lars, in *Economic Effects of Biofuel Production*, ed. B. Marco Aurélio dos Santos, IntechOpen, Rijeka, 2011, ch. 8, DOI: [10.5772/17198](https://doi.org/10.5772/17198).

42 S. Adamopoulos, E. Voulgaridis and C. Passialis, *Holz Roh-Werkst.*, 2005, **63**, 327–333.

43 U. Sahlberg, L. Salmén and A. Oscarsson, *Wood Sci. Technol.*, 1997, **31**, 77–86.

44 D. Ellinger and C. A. Voigt, *Ann. Bot.*, 2014, **114**, 1349–1358.

45 F. C. Bao, Z. H. Jiang, X. M. Jiang, X. X. Lu, X. Q. Luo and S. Y. Zhang, *Wood Sci. Technol.*, 2001, **35**, 363–375.

46 R. Funada, H. Abe, O. Furusawa, H. Imaizumi, K. Fukazawa and J. Ohtani, *Plant Cell Physiol.*, 1997, **38**, 210–212.

47 J. C. Mortimer, G. P. Miles, D. M. Brown, Z. Zhang, M. P. Segura, T. Weimar, X. Yu, K. A. Seffen, E. Stephens, S. R. Turner and P. Dupree, *Proc. Natl. Acad. Sci. U. S. A.*, 2010, **107**, 17409–17414.

48 R. L. Silveira, S. R. Stoyanov, S. Gusarov, M. S. Skaf and A. Kovalenko, *J. Am. Chem. Soc.*, 2013, **135**, 206–211.

49 T. E. Timell, *Wood Sci. Technol.*, 1967, **1**, 45–70.

50 A. Teleman, M. Nordström, M. Tenkanen, A. Jacobs and O. Dahlman, *Carbohydr. Res.*, 2003, **338**, 525–534.

51 M. G. Handford, T. C. Baldwin, F. Goubet, T. A. Prime, J. Miles, X. Yu and P. Dupree, *Planta*, 2003, **218**, 27–36.

52 J. S. Kim and G. Daniel, *Planta*, 2012, **236**, 1275–1288.

53 P. M.-A. Pawar, M. Derba-Maceluch, S.-L. Chong, M. L. Gandla, S. S. Bashar, T. Sparrman, P. Ahvenainen, M. Hedenström, M. Özparpucu, M. Rüggeberg, R. Serimaa, M. Lawoko, M. Tenkanen, L. J. Jönsson and E. J. Mellerowicz, *Biotechnol. Biofuels*, 2017, **10**, 98.

54 L. Donaldson, *Wood Sci. Technol.*, 2007, **41**, 443–460.

55 L. A. Donaldson, *Wood Sci. Technol.*, 1994, **28**, 111–118.

56 J. J. Lyczakowski, M. Bourdon, O. M. Terrett, Y. Helariutta, R. Wightman and P. Dupree, *Front. Plant Sci.*, 2019, **10**, 1398.

57 I. Duchesne, E. Hult, U. Molin, G. Daniel, T. Iversen and H. Lennholm, *Cellulose*, 2001, **8**, 103–111.

58 E. L. Hult, P. T. Larsson and T. Iversen, *Polymer*, 2001, **42**, 3309–3314.

59 J. Fromm, in *Cellular Aspects of Wood Formation*, ed. J. Fromm, Springer Berlin Heidelberg, Berlin, Heidelberg, 2013, pp. 3–39, DOI: [10.1007/978-3-642-36491-4\\_1](https://doi.org/10.1007/978-3-642-36491-4_1).

60 J. Široký, R. S. Blackburn, T. Bechtold, J. Taylor and P. White, *Cellulose*, 2010, **17**, 103–115.

61 S. Collazo-Bigliardi, R. Ortega-Toro and A. Chiralt-Boix, *Carbohydr. Polym.*, 2018, **191**, 205–215.

62 R. Moriana, F. Vilaplana and M. Ek, *Carbohydr. Polym.*, 2016, **139**, 139–149.

63 R. Requena, A. Jiménez-Quero, M. Vargas, R. Moriana, A. Chiralt and F. Vilaplana, *ACS Sustainable Chem. Eng.*, 2019, **7**, 13167–13177.

64 S. Park, J. O. Baker, M. E. Himmel, P. A. Parilla and D. K. Johnson, *Biotechnol. Biofuels*, 2010, **3**, 10.

65 M. Derba-Maceluch, F. Amini, E. N. Donev, P. M. A. Pawar, L. Michaud, U. Johansson, B. R. Albrechtsen and E. J. Mellerowicz, *Front. Plant Sci.*, 2020, **11**, 651.

